Eur J Med Res (2010) 15: 152-161

Enhanced Effect of Soluble Transforming Growth Factor-β Receptor II and IFN-γ Fusion Protein in Reversing Hepatic Fibrosis

H. Yao[1], J. Pan[2], Y. Qian[3], Z. Pei[3], A. Bader[4], N. H. Brockmeyer[4], P. Altmeyer[4], L. Zhang[3]

[1]State Key Laboratory for Diagnosis and Treatment of Infectious Diseases, the First Affiliated Hospital,
[2]Department of Microbiology and Parasitology, [3]Institute of Immunology,
Zhejiang University School of Medicine, China,
[4]Department of Dermatology and Allergy, Ruhr-University, Bochum, Germany

Abstract
Objective: To examine the in vivo anti-fibrotic effect of rat soluble transforming growth factor β receptor II (RsTβRII) and IFN-γ fusion protein (RsTβRII-IFN-γ) in rat hepatic fibrosis model.
Methods: Model rats were divided into five groups and treated i.m. for 8 weeks: 1) fibrotic model group (each rat, 100μl of 0.9% NaCl day^{-1}); 2) RsTβRII-IFN-γ treatment group (each rat, 0.136 mg · day^{-1}); 3) IFN-γ treatment group (each rat, 7.5 MU · day^{-1}); 4) RsTβRII treatment group (each rat, 0.048mg · day^{-1}); and 5) mixture of IFN-γ and RsTβRII treatment group (each rat, IFN-γ 7.5 MU · day^{-1}+ RsTβRII 0.048 mg · day^{-1}). After treatment, hepatic fibrogenesis was evaluated by histopathological analysis and measurement of collagen III, α-smooth muscle actin (α-SMA), TGF-β1, TGF-βRII and their mRNA.
Results: Immunohistochemistry, Western blot and real-time RT-PCR showed that RsTβRII-IFN-γ treatment significantly inhibited liver expression of collagen III, α-SMA, TGF-β1 and TGF-βRII at both protein and mRNA levels. Histopathological analysis also showed that the enhanced anti-fibrotic effects were achieved in model rats treated with RsTβRII-IFN-γ.
Conclusion: Our results confirmed that RsTβRII-IFN-γ has the enhanced effects in reversing hepatic fibrosis.

Key words: TGF-βRII; IFN-γ; Recombinant fusion protein; Hepatic fibrosis

Abbreviations: ECM: extracellular matrix; HSC: hepatic stellate cells; TGF-β: transforming growth factor-β; IFN-γ: interferon-γ; TGF-βRII: TGF-β type II receptor; sTGF-βRII: soluble TGF-β type II receptor; RsTβRII: rat soluble TGF-β type II receptor; RsTβRII-IFN-γ: rat soluble TGF-β type II receptor and IFN-γ fusion protein; VSV: vesicular stomatitis virus; Col III: collagen III; α-SMA: α-smooth muscle actin

Introduction

Liver fibrogenesis represents the common response of the liver to toxic, infectious, or metabolic agents and is characterized by increased synthesis and deposition of newly formed extracellular matrix (ECM) components [1]. Activated hepatic stellate cells (HSC) are known to be the primary ECM-producing cells in hepatic fibrogenesis [2]. An important role in fibrogenesis has been assigned to transforming growth factor (TGF)-β; TGF-β is in turn found in increased quantities in the injured liver, particularly after chronic liver injury [3]. The TGF-β superfamily consists of multiple family members, including the highly homologous TGF-β (TGF-β1, TGF-β2, and TGF-β3) isoforms, among of which TGF-β1 has prominent fibrogenic properties [4, 5], because TGF-β1 plays an important role in the activation of HSC which is the critical and fundamental event in hepatic fibrogenesis [6, 7]. Stellate cell activation is associated not only with enhanced production of all forms of ECM but also with up-regulation of cytoskeletal proteins, cytokines, and various cell surface receptors [8]. TGF-β stimulates collagen I mRNA transcription and increases its stability in activated stellate cells [9].

In mammalian cells, TGF-β response is mediated by type I and type II cell surface receptors that signal via cytoplasmic serine/threonine kinase domains [10]. TGF-β type II receptors (TGF-βRII) are constitutively active kinases that lead to ligand-binding specific signaling. TGF-βRII docking leads to TGF-β type I receptor recruitment, phosphorylation, and subsequent cellular signaling. TGF-βRII mediated signaling leads to pleiotropic effects in the wound healing response [11, 12].

Because the prominent role of TGF-β in hepatic fibrogenesis, a number of approaches have been used to abrogate the effect of TGF-β. Qi et al. used an adenoviral vector expressing a truncated TGF-βRII that can competitively bind to free TGF-β with membrane surface receptors to inhibit the effect of TGF-β on HSC [13]. Yata et al. used soluble TGF-βRII (sTGF-βRII) protein to treat hepatic fibrosis in mice and elucidated a dose-response relationship between the degree of inhibition of TGF-β and fibrogenesis [14]. Nakamuta et al. found that remote delivery and expression of sTGF-βRII in muscle prevented hepatic fibrosis in rats [15]. Additionally, development of a chimeric soluble TGF-β receptor, which binds free TGF-β and

thus inhibits its effects, has been shown to reduce fibrogenesis acutely after liver injury in rats [16].

It was found that IFN-γ can induce the expression of Smad7, inhibit the interaction between TGF-β complex and Smad3, which indirectly inhibits TGF-β activity and HSC activation [17, 18]. Because sTGF-βRII and IFN-γ act at different sites to block the activity of TGF-β and the activation of HSC, combined application of them may produce a synergic effect and in turn reduce their required dose to lower the side effect.

In our previous study, we constructed an recombinant plasmid expressing a bioactive fusion protein (RsTβRII-IFN-γ) that comprises rat sTGF-βRII (RsTβRII) and IFN-γ in mammalian cells and showed that the purified RsTβRII-IFN-γ could antagonize the proliferation-inhibitive effect of TGF-β1 on Mink lung epithelial (Mv1Lu, CCL-64) cells and inhibit HSC activation in vitro [19]. In the present study, we investigated the in vivo anti-fibrotic effects of RsTβRII-IFN-γ fusion protein in a rat model with hepatic fibrosis.

Materials and Methods

Amplification and Purification of the RsTβRII-IFN-γ Fusion Protein

Clones expressing the highest levels of RsTβRII-IFN-γ fusion protein were selected for production of the fusion protein. RsTβRII-IFN-γ fusion protein was purified from culture supernatant by protein A-Sepharose affinity chromatography under sterile and endotoxin free conditions. The protein is greater than 95% pure as judged by sodium dodecyl sulfate/polyacrylamide gel electrophoresis and contains less than 1 unit endotoxin per milligram protein.

RsTβRII-IFN-γ Fusion Protein Antiviral Assay

Antiviral assay was performed as described by Pan et al. [20] with minor modification. 1×10^4 L929 cells (100μl) per well were added to a 96-well microtiter tissue culture plate. The cells were incubated at 37 °C in 5%CO_2 condition and 100μl serial dilutions of RsTβRII-IFN-γ fusion protein in which RsTβRII activity has been blocked by its neutralizing antibody were added to the assay plate except for the normal and viral controls after the cells adhered to wells. After 3 hours, 25μl of vesicular stomatitis virus (VSV) was added to the assay plate except for the normal controls. The cells were incubated for 24 hours totally and 10μl MTT (5mg/ml) were added to each well 6 hours before the end of the culture. After centrifugation at 1000rpm for 5 minutes, supernatants were removed. The cells were then lysed in 150μl dimethyl sulfoxide (DMSO). The absorbance at 570 nm was measured and percent protection of L929 cells from infection of VSV was calculated. Each assay was carried out in triplicate.

Mink Lung Epithelial Cell Proliferation Assay

The Mv1Lu cell line, CCL64 cells, were maintained in minimal essential medium supplemented with 100 units/ml penicillin, 100 μg/ml streptomycin, and 10% fetal bovine serum. Serial dilutions of RsTβRII-IFN-γ fusion protein in which IFN-γ activity has been blocked by its neutralizing antibody were incubated with 800 pg/ml TGF-β1 for one hour in assay medium in a 96-well plate. 1×10^4cells of CCL64 were added into each well. The cells were incubated at 37 °C for 72 hours and 10μl MTT (5mg/ml) were added into each well 4 hours before the end of the culture. After centrifugation at 1000rpm for 5 minutes, supernatants were removed. The cells were then lysed in 150μl DMSO. The absorbance which reflects cell proliferation was measured at 570 nm. Each assay was carried out in triplicate.

Construction, Purification, and Activity of the RsTβRII Protein

RsTβRII genes were amplified from rat liver cDNA with specific primers as previously described [19]. The RsTβRII fragment was digested with HindIII/BamHI restriction enzymes, then cloned into the pSecTag2 expression vector. The ultimate construct was screened by ampicillin and identified by double enzyme digestion and DNA sequencing. Transfection of the pSecTag2/RsTβRII into CHO was conducted with liposomes and the stable expression strains were screened with Zeocin®. The supernatants of transfected CHO were examined by Western blotting for RsTβRII expression. The purification and activity testing of the RsTβRII protein were performed as described for RsTβRII-IFN-γ fusion protein.

Animal Model with Hepatic Fibrosis and Treatment

Sprague-Dawley rats (n = 210, provided by Zhejiang University Experimental Animal Center) weighing 135g-150g were used. Principles of laboratory animal care (NIH publication No. 86-23, revised 1985) were followed.

Hepatic fibrosis was induced by subcutaneous injection of CCl4 as described previously [21] with minor modification. Rats (n = 200, in addition, 10 rats were chosen as the normal control group, named group Nor.) were subcutaneously administered dissolved CCl4 in camellia oil (a proportion of 1:1) at 0.3ml/100 g of body weight, twice a week for 8 weeks. Five rats were killed at the end of each week to examine pathological changes of livers.

According to histological examination, hepatic fibrosis appeared at the end of the eighth week from the start of the study. 156 rats with hepatic fibrosis could be used for the study. Model rats were randomly divided into five groups: 1) fibrotic model group (n = 10) (group E, each rat, 100μl of 0.9% NaCl day^{-1}, i.m.); 2) RsTβRII-IFN-γ fusion protein treatment group (group A, each rat, 0.136mg (containing 7.5 MU IFN-γ and 0.048mg RsTβRII) · day^{-1}, i.m.); 3) IFN-γ treatment group (group B, each rat, 7.5MU · day^{-1}, i.m.); 4) RsTβRII protein treatment group (group C, each rat, 0.048mg · day^{-1}, i.m.); and 5) mixture of IFN-γ and RsTβRII treatment group (group D, each rat, IFN-γ 7.5MU · day^{-1}+ RsTβRII0.048mg · day^{-1}, i.m.).

The latter four groups were given, every two days for totally 8 weeks, RsTβRII-IFN-γ fusion protein, IFN-γ, RsTβRII protein, mixture of IFN-γ and RsTβRII protein, respectively. Rats in the fibrotic model group were given 0.9% sodium chloride by intramuscular injection. Rats in the normal control group didn't receive any treatment.

Four weeks after the finish of treatment, rats of each group were killed, and histological sections of their livers were evaluated by hematoxylin and eosin and Sirius red stains. Expressions of collagen III (Col III), α-smooth muscle actin (α-SMA), TGF-β1 and TGF-βRII were examined with immunohistochemistry, Western blotting and real-time RT-PCR.

Histopathological Analysis

Livers were fixed in 10% neutral formalin, embedded in paraffin, sectioned, and stained with hematoxylin-eosin and Sirius red respectively. Sirius red staining method was used to specifically stain fibrous tissue components. For Sirius red staining, the sections were incubated for 30 minutes in 0.1% Sirius red F3B containing saturated picric acid and 0.1% Fast Green (Sigma Chemical Co., St. Louis, MO). After rinsing twice with distilled water, sections were briefly dehydrated with anhydrous alcohol and coverslipped. Collagen stained with Sirius red was quantitated in the sections that were randomly chosen (under 20× magnification; 10 fields each from 8 different rats for a total of 80 fields for each group) with Meta-View software (Universal Imaging Corp., Downington, PA). These sections were observed under polarization microscope (Leica DMLB, Leica Wetalar, Germany) to distinguish type I and III collagen [22].

Immunohistochemistry Analysis

For measurement of Col III, α-SMA and TGF-β1, liver tissues were fixed in formalin, embedded in paraffin wax, and 5-μm sections were cut and stained using the immunohistochemical Streptavidin biotin-peroxidase complex (SABC) method as described previously with minor modification [23, 24].

Real-time PCR

Frozen rat's liver tissue, stored at -80 °C, were shattered in liquid nitrogen and total RNA was isolated by the RNAeasy isolation kit (Qiagen) according to the manufacturer's instructions. First-strand cDNA was synthesized. Real-time reverse transcriptase (RT)-PCR was performed as described by Li et al. [25]. Briefly, a real-time PCR was performed using Light Cycler FastStart SYBR Green I Master (Roche) according to the manufacturer's instructions. Synthesized cDNA then served as a template in the following quantitative PCR reaction. Primer sequences were designed as follows: Col III (220bp): forward 5'-TGGTCCTCAGGGTG TAAAGG-3', reverse 5'-GTCCAGCATCA CCTTT TGGT-3'; α-SMA (457bp): forward 5'-AGGGAGTA ATGGTTGGAATGGG -3' , reverse 5'-GGAGTACG GTACGC AGA-3'; TGF-β1 (404bp): forward 5'-CA CCAT CCATGACATGAACC-3', reverse 5'-TCATG TTGGACAACTGCTCC-3'; and TGF-βRII (560bp): forward 5'-CGTGTGGAGGAAGAACAACA-3', reverse 5'-TCTC AAACTGCTCTGAGGTG-3'; β-actin (619 bp): forward 5'-CGCTG CGCTGGTCGTC GA CA-3', reverse 5'-GTCACGCACGATTTCCCGCT-3'. β-actin was used as an internal standard. Each Light Cycler PCR reaction system (15μl) included: 1.5 μl of Light Cycler FastStart DNA Master Mix, 1.8μl of MgCl2 (25mM), 0.4μl of each primer (10μM), 2μl of 1:10 diluted cDNA, 9.3μl of H_2O. The reactions started at 95 °C for 10 minutes followed by 50 cycles at 94 °C for 10 seconds, 65 °C for 15 seconds, 72 °C for 15 seconds. PCR products were denaturalized for 1min at 95 °C before rapidly chilling to 55 °C for 30 seconds. Melting peaks of PCR products were determined by heat-denaturing them over a 40 °C temperature gradient at 0.1 °C/s from 55°C to 95 °C. Reaction specificity was confirmed by 1.5% gel electrophoresis of products after real-time PCR and melting curve analysis. Ratios of Col III/β-actin, α-SMA/β-actin, TGF-β1/β-actin, TGF-βRII/β-actin, and mRNA were calculated for each sample and expressed as the means ± SEM.

Westernblot Analysis

Western blot analysis of Col III, α-SMA, TGF-β1, TGF-βRII and β-actin in the liver was performed as previously described [26].

Results

RsTβRII-IFN-γ Fusion Protein Can Protect L929 from Infection of VSV

Anti-viral activity is one of the biological characteristics of IFN-γ [14, 27]. We tested if RsTβRII-IFN-γ fusion protein could protect L929 cells from infection

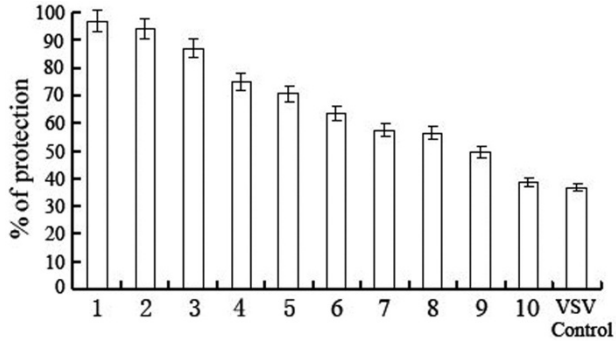

Fig. 1. RsTβRII-IFN-γ dose-dependently protects L929 cells from infection of VSV. 1×10^4/ well L929 cells were added into a 96-well plate. Serial dilutions of RsTβRII-IFN-γ fusion protein were added into the assay plate except for the normal and viral controls after the cells adhered to wells. 3 hours later, 25μl of VSV was added into each well except for the normal controls. The cells were incubated for 24 hours totally and 10μl MTT (5mg/ml) were added into each well 4 hours before the end of the culture. The cells were lysed in 150μl DMSO. The absorbance at 540nm was measured and percent protection of L929 from infection of VSV was calculated. Each assay was carried out in triplicate. 1: original RsTβR-IFN-γ fusion protein; 2~10: 2×serial dilutions of 1; VSV Control: L929 challenged by VSV

of VSV by anti-viral assay. We found that L929 cells quickly exhibited typical signs of VSV infection in the absence of RsTβRII-IFN-γ, however, in the presence of RsTβRII-IFN-γ, L929 cells became insensitive to VSV challenge, and this protective effect is dose-dependent (Fig. 1), indicating that RsTβRII-IFN-γ fusion protein retains the anti-viral activity of IFN-γ.

Recombinant RsTβRII-IFN-γ Fusion Protein Can Antagonize the Activity of TGF-β1 in vitro

It was demonstrated that sTGF-βRII could antagonize the bioactivity of TGF-β1 to inhibit the proliferation of mink lung epithelial cells [14]. We tested if RsTβRII-IFN-γ has the bioactivity of sTGF-βRII by a mink lung epithelial cell proliferation assay. As shown in Figure 2, when TGF-β1 was added to the media, proliferation of CCL-64 was inhibited. While different concentration of RsTβRII-IFN-γ fusion protein and same quantity of TGF-β1 were incubated together with CCL-64 cells for 72 hours, TGF-β1 mediated inhibition of proliferation was blocked by RsTβRII-IFN-γ fusion protein in a dose-dependent manner, suggesting that RsTβRII-IFN-γ retains RsTβRII bioactivity.

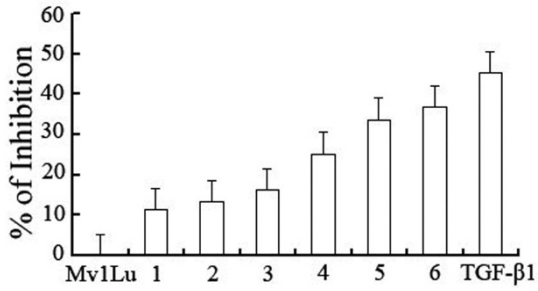

Fig. 2. RsTβRII-IFN-γ fusion protein blocks the inhibitory effect of TGF-β1 on CCL-64 cell proliferation. Serial dilutions of RsTβRII-IFN-γ fusion protein were incubated with 800 pg/ml TGF-β1 for one hour in assay medium in a 96-well plate. 1×10^4 cells of CCL-64 per well were added into each well. The cells were incubated at 37 °C for 72 hours and 10μl MTT (5mg/ml) were added into each well 4 hours before the end of the culture. The cells were lysed in 150μl DMSO. The absorbance at 540 nm was measured. Each assay was carried out in triplicate. Mv1Lu: Untreated CCL-64 cells. 1: Original purified RsTβRII-IFN-γ fusion protein; 2~6: 2×serial dilutions of 1; TGF-β1: CCL-64 cells treated with TGF-β1 without RsTβRII-IFN-γ fusion protein

RsTβRII Can Neutralize the Growth-inhibitory Effect of TGF-β1 on Mink Lung Epithelial Cells

To identify the bioactivity of the RsTβRII, we performed a mink lung epithelial cell proliferation assay. As shown in Figure 3, RsTβRII dose-dependently inhibited the growth-inhibitory effects of TGF-β1 on CCL64 cells, implying that RsTβRII we prepared could competitively bind to TGF-β1 with the membrane TGF-βRII, hereby inhibiting the bioactivity of TGF-β1.

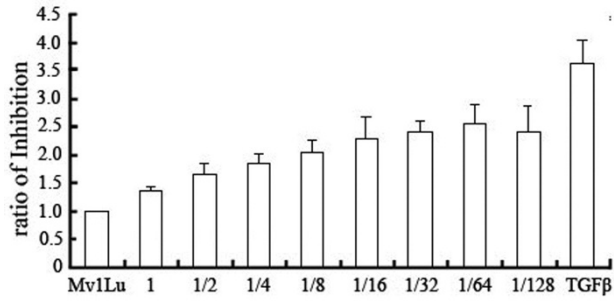

Fig. 3. RsTβRII blocks the growth-inhibitory effect of TGF-β1 on CCL-64 cells. Serial dilutions of RsTβRII were incubated with 800 pg/ml TGF-β1 for one hour in assay medium in a 96-well plate. 1×10^4 cells of CCL-64 per well were added into each well. The cells were incubated at 37 °C for 72 hours and 10μl MTT (5mg/ml) were added into each well 4 hours before the end of the culture. The cells were lysed in 150μl DMSO and the absorbance at 540 nm was measured and ratios of inhibition were calculated. Mv1Lu: Untreated CCL-64 cells; 1: Original purified RsTβR protein; TGF-β1: CCL-64 cells treated with TGF-β1 but without RsTβRII protein.

RsTβRII-IFN-γ Fusion Protein Treatment Reverses Hepatic Fibrosis

Histological examination of livers from normal rats (group Nor) demonstrated that ECM deposition was present only in portal and central areas (Fig. 4Nor). Hematoxylin-eosin staining of liver sections from untreated rats with hepatic fibrosis (group E) exhibited periportal, pericentral, and central-central, portal-portal, and portal-central matrix deposition and numerous granulomas containing a diffuse array of inflammatory cells, within an invasive collagen network (Fig. 4E). In contrast, livers from rats with hepatic fibrosis treated with RsTβRII-IFN-γ fusion protein, IFN-γ, RsTβRII, and mixture of IFN-γ and RsTβRII, respectively (group A, B, C and D) showed much less granulomas in which only a few cells were found, and markedly decreased collagen (Fig. 4A, B, C and D).

Quantitative morphometric assessment of fibrosis (identified by Sirius red staining) showed a significant reduction in fibrogenesis after treatment of rats with RsTβRII-IFN-γ fusion protein, IFN-γ, RsTβRII, and mixture of IFN-γ and RsTβRII, respectively (Figs. 4A, B, C and D). Sirius red staining showed that a little collagen deposition in the portal tracts and lobules was seen in livers from rats with hepatic fibrosis treated by RsTβRII-IFN-γ fusion protein. Furthermore, only collagen fibers around the terminal hepatic veins were observed (Fig. 4A). Collagen depositions in liver sections from rats treated with IFN-γ, RsTβRII or RsTβRII+IFN-γ. respectively were particularly evident, but only thin bands of collagen which formed short, incomplete septum could be seen (Figs. 4B, C and D).

Taken together, the most effective anti-fibrotic effect was achieved in model rats treated with RsTβRII-IFN-γ fusion protein.

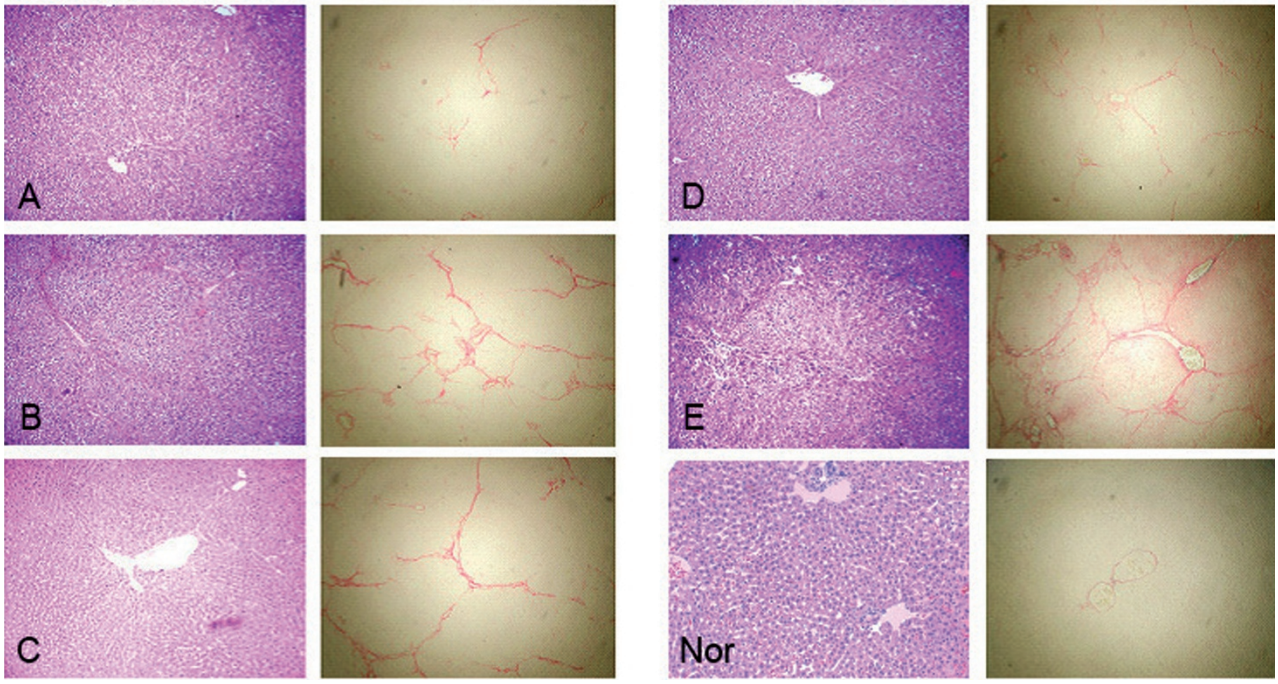

Fig. 4. Histopathological analyses of livers in rats from different groups. 4 weeks after the finish of treatment, rats with hepatic fibrosis in each group were killed and livers were harvested, fixed in 10% neutral formalin, sectioned, and stained with hematoxylin-eosin (left column) and Sirius red (right column) respectively. Representative micrograph in each group was shown (original magnification ×200). A, RsTβRII-IFN-γ fusion protein treatment group; B, IFN-γ treatment group; C, RsTβRII treatment group; D, mixture of IFN-γ and RsTβRII treatment group; E, fibrotic model group; Nor, normal control group.

◀ 5A

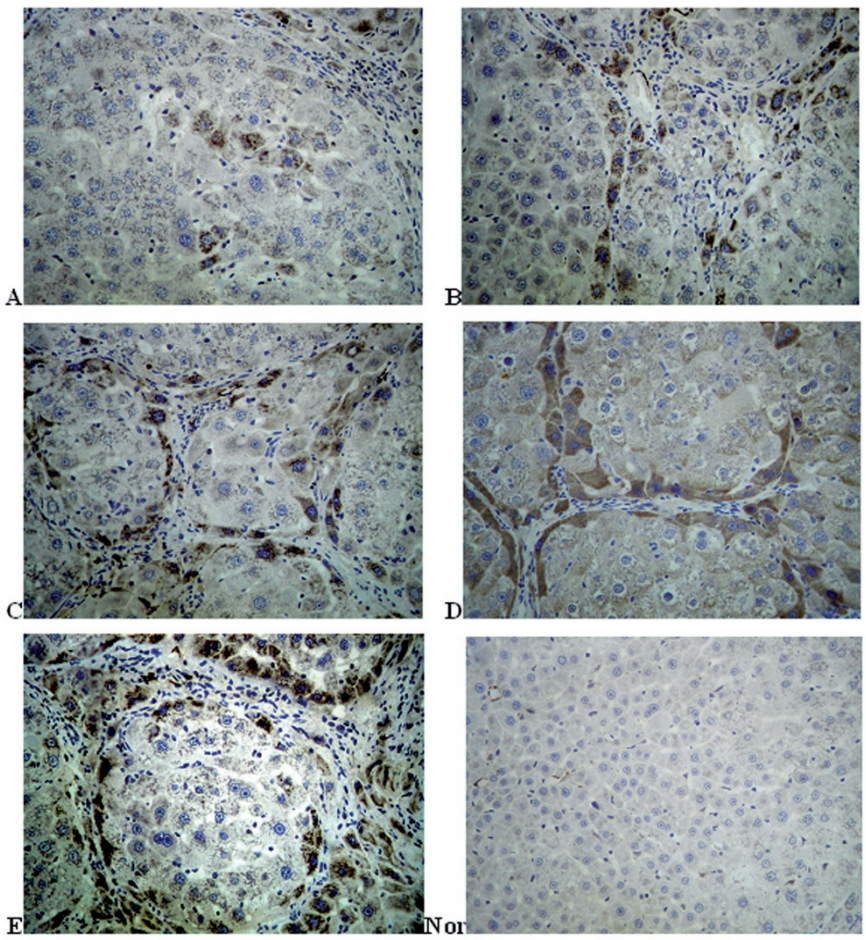

Fig. 5. Immunohistochemistry of α-SMA, Col III, TGF-β1. Paraffin sections of liver were incubated overnight at 4°C with anti-α-SMA (Fig. 5A), anti-type III collagen (Fig. 5B), anti-TGF-β1 (Fig. 5C) monoclonal antibodies (1:100 dilutions). This was followed by incubation in biotinylated goat anti-mouse antibodies (1:200 dilutions) for 40 min and treated with SABC for 30 min at 37 °C. The peroxidase activity, which resulted in a brown staining of cytoplasmic reaction sites, was visualized by incubation for 30 sec~1 min in dimethylbenzidine and staining lightly with hematoxylin.

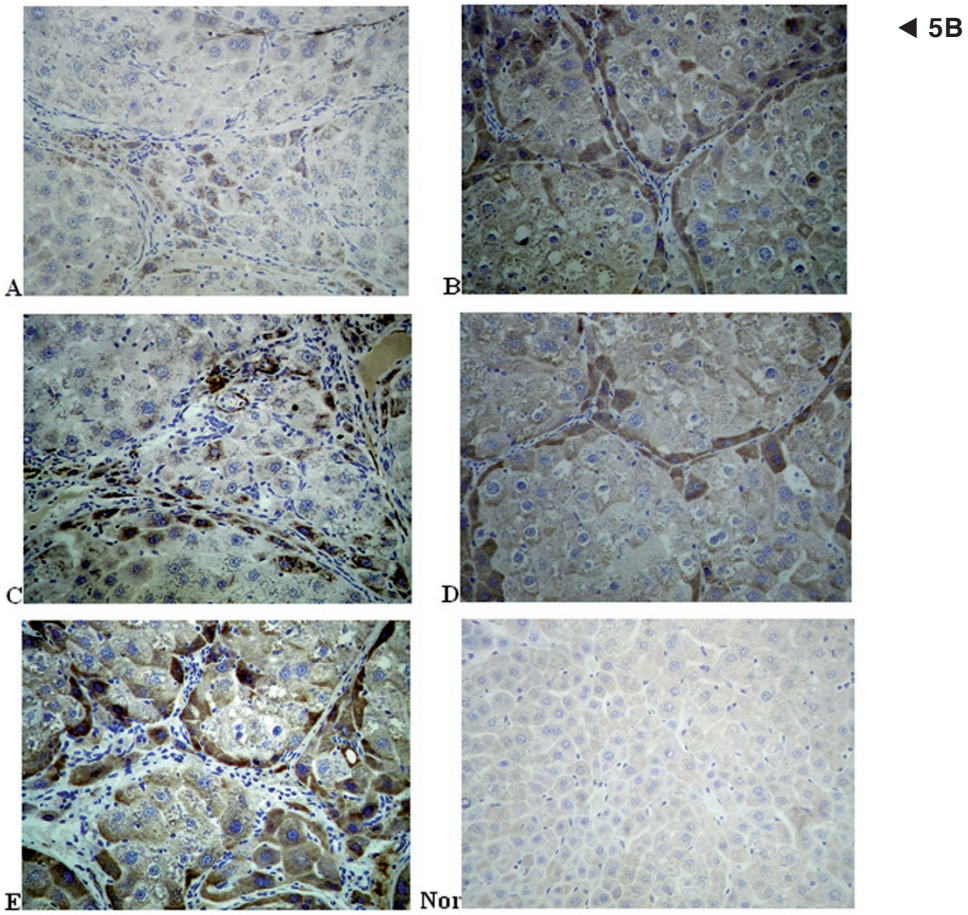

◀ 5B

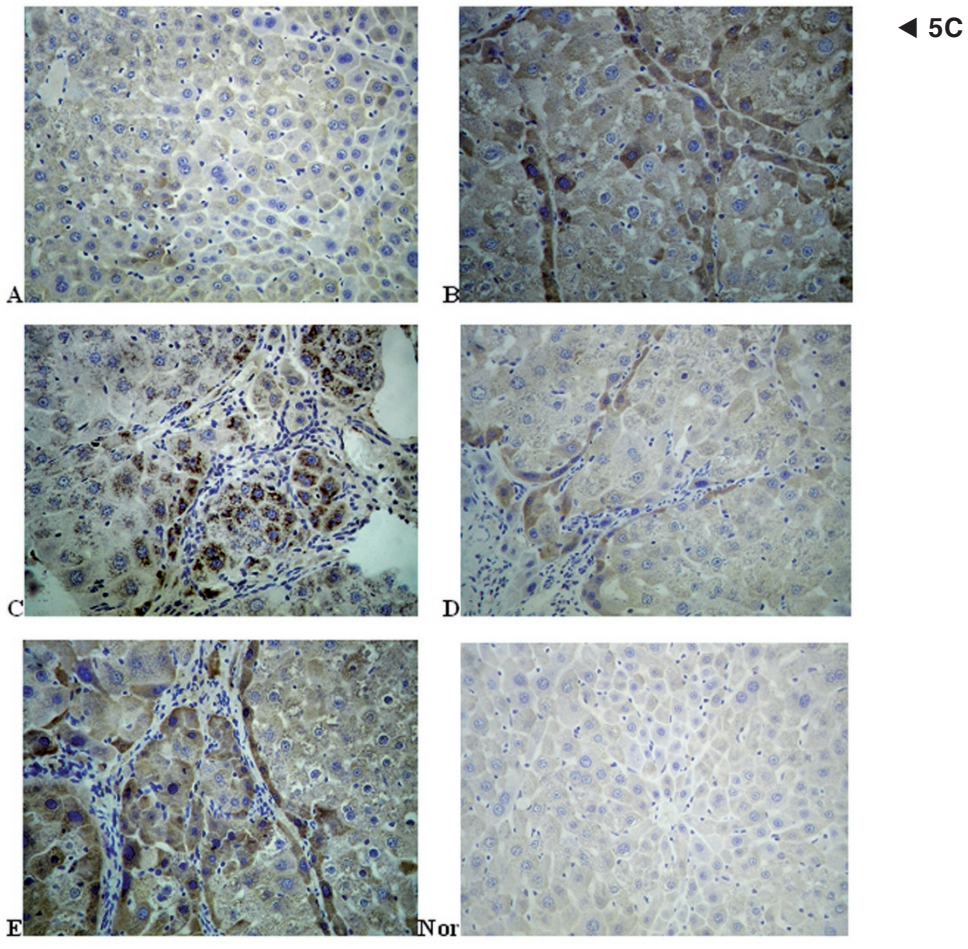

◀ 5C

RsTβRII-IFN-γ Fusion Protein Treatment Reduces Expression of α-SMA, Col III, TGF-β1 and TGF-βRII

Immunohistochemistry analyses of the liver further revealed the striking differences. As shown in Figures 5A, in the normal control group (Group Nor), α-SMA positive cells were detected mainly in the portal space as elements of vascular walls or as fibroblastlike cells scattering in the connective tissue or near bile ductules. In lobule, α-SMA positive cells were present on the walls of large and medium sized terminal hepatic veins. The pattern of distribution of α-SMA positive cells was modified in liver injured rats as compared with the normal control rats. In rats with hepatic fibrosis (group E), α-SMA positive cells were detected in portal space, sinusoid, lobule and areas where fibrotic septum appeared. Distributions of α-SMA positive cells in liver from rats with hepatic fibrosis treated with RsTβRII-IFN-γ fusion protein, IFN-γ, RsTβRII or RsTβRII +IFN-γ respectively were all reversed when compared with those of hepatic fibrosis model rats. After 8 weeks of RsTβRII-IFN-γ fusion protein treatment (group A), only thin and incomplete parenchymal α-SMA positive septum joining thickened centrilobular veins were observed in liver sections. α-SMA positive cells were mainly found in portal space and areas around fibrotic septum. Few α-SMA positive cells were present in sinusoid and lobule (Fig. 5A). Moreover, it was obvious that the greatest anti-fibrotic effect was achieved by treatment with RsTβRII-IFN-γ fusion protein in accordance with the histopathological analysis (Fig. 4A). The deposition and distribution range of positive staining for Col III in livers from rats with hepatic fibrosis treated by RsTβRII-IFN-γ fusion protein mirrored the same trend as α-SMA (Fig. 5B).

As TGF-β1 is an profibrogenic cytokine that signals through a receptor consisting of type I and type II components [28], the expression of TGF-β1 in livers from different groups was also examined by immunohistochemistry. As shown in Figure 5C, normal rat livers showed light, positive staining which was scattered in the perivascular spaces, around portal tracts. Livers from rats with hepatic fibrosis showed a marked increase in positive staining for TGF-β1, with the reactivity primarily occurring in the portal tract area and granulomas. However, livers from rats with hepatic fibrosis treated with RsTβRII-IFN-γ fusion protein, IFN-γ, RsTβRII, and mixture of IFN-γ and

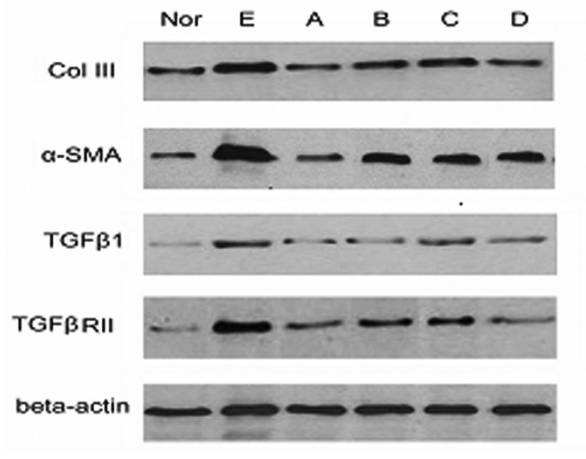

Fig. 6. Western blotting analysis of Col III, α-SMA, TGF-β1 and TGF-βRII. Liver tissues from rats in different groups were lysed in the lysis buffer. Samples were centrifuged to pellet cell debris, mixed with SDS-PAGE sample buffer. After boiled for 5~10 min, 40 μg of protein was electrophoresed on a 10% SDS-polyacrylamide gel. The protein was transferred to PVDF membrane. The blots were incubated with the primary antibody against Col III, α-SMA, TGF-β1, TGF-βRII and β-actin (1 : 400) at 4°C overnight respectively and subsequently with corresponding secondary antibody (1 : 1000) at room temperature for 2 h. Protein bands were visualized with an ECL Western blotting detection system kit and signal was captured on X-ray film.

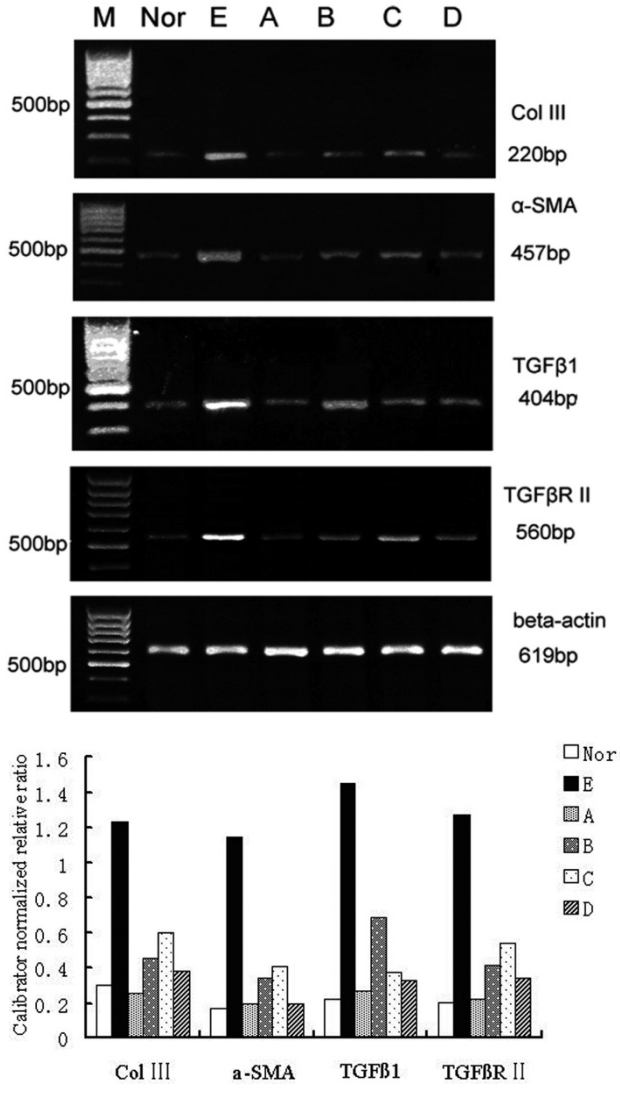

Fig. 7. Real-time RT-PCR for Col III, α-SMA, TGF-β1 and TGF-βRII mRNA expression. Total RNA was isolated from frozen liver tissues. Real-time RT-PCR was performed using Light Cycler FastStart SYBR Green I Master according to the manufacturer's instructions. (A) Gel electrophoresis of PCR products. (B) Calibrator normalized relative ratios. A: RsTβRII-IFN-γ fusion protein treatment group; B: IFN-γ treatment group; C: RsTβRII protein treatment group; D: mixture of RIFN-γ and RsTβRII treatment group; E: fibrotic model group; Nor: normal control group.

RsTβRII respectively (group A, B, C and D) showed decreased expression of TGF-β1. Moreover, liver sections from rats with hepatic fibrosis treated with RsTβRII-IFN-γ fusion protein (group A) showed marked decrease in expression of TGF-β1 when compared with those from rats with hepatic fibrosis treated with IFN-γ, RsTβRII and mixture of IFN-γ and RsTβRII, respectively (group B, C and D) although the distribution pattern of positive cells was similar to that of the hepatic fibrotic model group (group E).

Western blotting analyses of collagen III, α-SMA, TGF-β1 and TGF-βRII content in livers of different groups also substantiated the histological impression, showing decreased contents of Col III, α-SMA, TGF-β1 and TGF-βRII in livers from rats with hepatic fibrosis treated by RsTβRII-IFN-γ fusion protein, IFN-γ, RsTβRII, and mixture of IFN-γ and RsTβRII, respectively (Fig. 6). However, the most effective therapeutic effect was achieved again by treatment with RsTβRII-IFN-γ fusion protein.

Finally, we investigated the mRNA expression of Col III, α-SMA, TGF-β1 and TGF-βRII in livers of different groups. As shown in Figure 7, 4 weeks after the stop of treatment, there was an increase in TGF-β1 mRNA expression in livers from rats with hepatic fibrosis, while only detectable level of TGF-β1 mRNA was shown in livers from normal control rats. This increase in TGF-β1 steady-state mRNA levels approximately paralleled the increase in Col III, α-SMA and TGF-βRII mRNA levels. Moreover, livers from rats with hepatic fibrosis treated with RsTβRII-IFN-γ fusion protein (group A) showed markedly decreased mRNA expression of Col III, α-SMA, TGF-β1 and TGF-βRII compared with untreated, hepatic fibrotic rats. In contrast, RsTβRII, IFN-γ or RsTβRII+IFN-γ treatment did not significantly alter steady-state mRNA levels for TGF-β1 and TGF-βRII (Fig. 7A and B). These data substantiated again the histological analyses, and demonstrated that RsTβRII-IFN-γ fusion protein treatment did inhibit collagen deposition.

Discussion

Hepatic fibrosis is a pathological process shared by a variety of causes in response to hepatocyte necrosis and inflammatory insults, which is mainly characterized by the excessive deposition of ECM in Disse space in the liver. Activated HSC are known to be the primary ECM-producing cells in hepatic fibrogenesis. The activation of HSC is largely mediated by TGF-β, which is actually the most potent profibrogenic cytokine. Thus the TGF-β/HSC axis is widely considered a potential target for anti-hepatic-fibrosis therapy by many investigators. TGF-β exhibits its biological function via the TGF-β receptors, including type I, II and III receptors. Both the dominant-negative TGF-βRII and sTGF-βRII have been proved to be anti-fibrosis, they can bind to TGF-β but lack the intracellular kinase domain which is essential to initiate signal transduction[29, 30]. IFN-γ inhibits the interaction between TGFβR complex and Smad3 by blocking TGF-β signaling via JAK/STAT pathway, thus antagonizing the fibrogenic effect[31]. Neutralizing the effect of TGF-β in vivo leads to reduced ECM deposition in both the liver [13~16] and other tissues [32]. Thus, the evidence linking TGF-β and fibrogenesis is substantial and, moreover, raises important possibilities for therapeutics targeted at this pathway.

Cytokine recombinant fusion protein refers to a category of artificial protein products produced by genetically fusing the encoding fragments of cytokines and/or other proteins with specific biological functions. This kind of protein exerts strongly enhanced biological activities when compared with the original individual proteins or mixed proteins. Because sTGF-βRII and IFN-γ act at different sites to block the activity of TGF-β and the activation of HSC, combined application of them may produce a synergic anti-fibrotic effect and in turn reduce their required dose to lower the side effect. So we prepared a novel RsTβRII-IFN-γ fusion protein by gene recombinant, and tested the bioactivity and the in vivo anti-fibrotic effects of RsTβRII-IFN-γ fusion protein.

At first, we showed that the growth-inhibitory effect of TGF-β on Mv1Lu epithelial cells was abrogated, in a dose-dependent manner, by RsTβRII-IFN-γ fusion protein, indicating that RsTβRII-IFN-γ fusion protein retains RsTβRII bioactivity. In anti-viral assay, L929 cells without RsTβRII-IFN-γ protection quickly exhibits the typical signs of VSV infection, while RsTβRII-IFN-γ protected L929 turned out to be insensitive to VSV challenge, and this protective effect is also dose-dependent, indicating that RsTβRII-IFN-γ retains the anti-viral activity of IFN-γ. Next, we investigate the in vivo anti-fibrotic effect of RsTβRII-IFN-γ fusion protein in rat model with hepatic fibrosis induced by subcutaneous injection of CCl4.

CCl_4 is one of the most widely used hepatic toxins for experimental induction of liver fibrotic cirrhosis in laboratory [21, 33, 34]. The model was used even in 1936. But, disadvantages of the model, such as higher mortality rate, were apparent. For this reason, 200 rats were used to produce CCl_4-iduced hepatic fibrosis model in our study. By histological examination of liver every week, we found that hepatic fibrosis was successfully induced at the eighth week. 156 rats in fibrotic model groups showed complete fibrotic septum, forming a pattern of micronodular cirrhosis and they were used for the following study.

As mentioned earlier, hepatic fibrosis is a pathological process which is mainly characterized by the excessive expression and deposition of ECM (especially Col I and III) [35] and activated HSC, characterized by the expression of α-SMA, is the main producer of ECM [36]. Moreover, Zhang et al. found that TGF-β1 and TGF-βRII play important roles in the pathogenesis of hepatic fibrosis [37]. Therefore, we used Col III, α-SMA, TGF-β1 and TGF-βRII expressions plus histopathological analysis as indices to evaluate the in vivo anti-fibrotic effects of RsTβRII-IFN-γ fusion protein. Our data showed that the pathological fibrosis scores were significantly lower in model rats treated with RsTβRII-IFN-γ fusion protein compared with other groups. In the mean time, liver contents and their distribution ranges of collagen III, α-SMA, TGF-β1 and TGF-βRII, as well as the expression of their mRNA decreased significantly in rats with he-

patic fibrosis treated with RsTβRII-IFN-γ fusion protein when compared with those of hepatic fibrosis control rats. These data suggest that the most prominent anti-fibrotic effect was achieved in rats with hepatic fibrosis treated with RsTβRII-IFN-γ fusion protein.

Taken together, our findings imply that RsTβRII-IFN-γ fusion protein might be a novel potential candidate in treating hepatic fibrosis. However, whether RsTβRII-IFN-γ fusion protein may cause any side effects when used to treat hepatic fibrosis needs further detailed investigation.

Acknowledgement: This work was supported by grants from National Research and Development Plan of High Technology (2001AA215111) and Science and Technology Foundation (2009C33150) and Natural Sciences Foundation (Y207419) of Zhejiang Provincial. We appreciate Dr. Bo Wang (Department of Pathology, First Affiliated Hospital, Zhejiang University School of Medicine) for his kind help in pathological analyses.

REFERENCES

1. Maher JJ, McGuire RF. Extracellular matrix gene expression increases preferentially in rat lipocytes and sinusoidal endothelial cells during hepatic fibrosis in vivo. J Clin Invest 1990, 86(5):1641-1648
2. Hsu YC, Chiu YT, Cheng CC, Wu CF, Lin YL, Huang YT. Antifibrotic effects of tetrandrine on hepatic stellate cells and rats with liver fibrosis. J Gastroenterol Hepatol 2007, 22(1): 99-111
3. Bissell DM, Wang SS, Jarnagin WR, Roll FJ. Cell-specific expression of transforming growth factor-beta in rat liver. Evidence for autocrine regulation of hepatocyte proliferation. J Clin Invest 1995, 96(1):447-455
4. Border WA, Ruoslahti E. Transforming growth factor-beta in disease: the dark side of tissue repair. J Clin Invest 1992, 90(1):1-7
5. Border WA, Noble NA. Transforming growth factor β in tissue fibrosis. N Eng J Med 1994, 331(19):1286-1292
6. Zhou X, Jamil A, Nash A, Chan J, Trim N, Iredale JP, Benyon RC. Impaired proteolysis of collagen I inhibits proliferation of hepatic stellate cells: implications for regulation of liver fibrosis. J Biol Chem 2006, 281(52): 39757-39765
7. Hellerbrand C, Stefanovic B, Giordano F, Burchardt ER, Brenner DA. The role of TGFbeta1 in initiating hepatic stellate cell activation in vivo. J Hepatol 1999, 30(1):77-87
8. Rockey DC. The cell and molecular biology of hepatic fibrogenesis. Clinical and therapeutic implications. Clin Liver Dis 2000, 4(2):319-355
9. Stefanovic B, Hellerbrand C, Holcik M, Briendl M, Aliebhaber S, Brenner DA. Posttranscriptional regulation of collagen alpha1(I) mRNA in hepatic stellate cells. Mol Cell Biol 1997, 17(9):5201- 5209
10. Massague J. TGF-beta signal transduction. Annu Rev Biochem 1998, 67:753-791
11. Border WA, Noble NA. Transforming growth factor beta in tissue fibrosis. N Engl J Med 1994; 331(19):1286-1292
12. Smith JD, Bryant SR, Couper LL, Vary CP, Gotwals PJ, Koteliansky VE, Linder V. Soluble transforming growth factor-beta type II receptor inhibits negative remodeling, fibroblast transdifferentiation, and intimal lesion formation but not endothelial growth. Circ Res 1999, 84(10):1212-1222
13. Qi Z, Atsuchi N, Ooshima A, Takeshita A, Ueno H. Blockade of type beta transforming growth factor signaling prevents liver fibrosis and dysfunction in the rat. Proc Natl Acad Sci USA 1999, 96(5):2345-2349
14. Yata Y, Gotwals P, Koteliansky V, Rockey DC. Dose-dependent inhibition of hepatic fibrosis in mice by a TGF-beta soluble receptor : implications for antifibrotic therapy. Hepatology 2002, 35(5):1022- 1030
15. Nakamuta M, Morizono S, Tsuruta S, Kohjima M, Kotoh K, Enjoji M. Remote delivery and expression of soluble type II TGF-beta receptor in muscle prevents hepatic fibrosis in rats. Int J Mol Med 2005, 16(1): 59-64
16. George J, Roulot D, Koteliansky VE, Bissell DM. In vivo inhibition of rat stellate cell activation by soluble TGF beta type II receptor: a potential new therapy for hepatic fibrosis. Proc Natl Acad Sci USA 1999, 96(22): 12719-12724
17. Zhang L, Mi J, Yu Y, Yao H, Chen H, Li M, Cao X. IFN-γ gene therapy by intrasplenic hepatocyte transplantation: a novel strategy for reversing hepatic Fibrosis in Schistosoma japonicum-infected mice. Parasite Immunology 2001, 23(1):11-17
18. Weng H, Mertens PR, Gressner AM, Dooley S. IFN-gamma abrogates profibrogenic TGF-beta signaling in liver by targeting expression of inhibitory and receptor Smads. J Hepatol 2007, 46(2): 295-303
19. Yu ZY, Zhang LH, Yao HP, Yang XH. Construction of the eukaryotic expression vector containing rat transforming growth factor beta type II receptor and interferon gamma fusion genes. J Zhejiang Univ (Medic Sci) 2005, 34(1):43-47
20. Pan J, Heiser A, Marget M, Steinmann J, Kabelitz D. Enhanced antimetastatic effect of fetal liver kinase 1 extracellular domain and interferon-gamma fusion gene-modified dendritic cell vaccination. Gene Ther 2005, 12(9): 742-750
21. Zhang Y, Ikegami T, Honda A, Miyazaki T, Bouscarel B, Rojkind M. Involvement of integrin-linked kinase in carbon tetrachloride-induced hepatic fibrosis in rats. Hepatology 2006, 44(3): 612-622
22. Zhang J, He JW, Wang TL, Zhao JB. Discriminate collagen type I and collagen type III by Sirius red stain and polarization microscopy. Zhonghua Binglixue Zazhi 1996, 25(3):180-181
23. Lortat-Jacob H, Baltzer F, Desmouliere A, Peyrol S, Grimaud JA. Lobular-but not periovular-inhibition of collagen deposition in the liver of S. mansoni infected mice using interferon-gamma. J Hepatol 1997, 26(4):894-903
24. Zhang LH, Pan JP, Yao HP, Sun WJ, Xia DJ, Wang QQ, He L, Wang J, Cao X. Intrasplenic transplantation of IL-18 gene-modified hepatocytes: an effective approach to reverse hepatic fibrosis in schistosomiasis through induction of dominant Th1 response. Gene Ther 2001, 8(17):1333-1342
25. Li JH, Wang W, Huang XR, Oldfield M, Schmidt AM, Cooper ME, Lan HY. Advanced glycation end products induce tubular epithelial-myofibroblast transition through the RAGE-ERK1/2 MAP kinase signaling pathway. Am J Pathol 2004, 164(4):1389-1397
26. Abergel A, Sapin V, Dif N, Chassard C, Darcha C, Marcand-Sauvant J, Gaillard-Martinie B, Rock E, Dechelotte P, Sauvant P. Growth arrest and decrease of alpha-SMA and type I collagen expression by palmitic acid in the rat hepatic stellate cell line PAV-1. Dig Dis Sci 2006, 51(5): 986-995
27. Pan J, Zhang M, Wang J, Wang Q, Xia D, Sun W, Zhang L, Yu H, Liu Y, Cao X. Interferon-g is an autocrine mediator for dendritic cell maturation. Immunol Lett 2004, 94(1-2): 141-151
28. Roulot D, Sevcsik AM, Coste T, Strosberg AD, Marullo S. Role of transforming growth factor beta type II receptor in hepatic fibrosis: studies of human chronic hepatitis C and experimental fibrosis in rats. Hepatology 1999, 29(6): 1730-1738

29. Cui X, Shimizu I, Lu G, Itonaga M, Inoue H, Shono M, Tamaki K, Fukuno H, Ueno H, Ito S. Inhibitory effect of a soluble transforming growth factor beta type II receptor on the activation of rat hepatic stellate cells in primary culture. J Hepatology 2003; 39(5):731-737
30. Ueno H, Sakamoto T, Nakamura T, Qi Z, Astuchi N, Takeshita A, Shimizu K, Ohashi H. A soluble transforming growth factor beta receptor expressed in muscle prevents liver fibrogenesis and dysfunction in rats. Hum Gene Ther 2000; 11(1):33-42
31. Ulloa L, Doody J, Massague J. Inhibition of transforming growth factor-β/SMAD signaling by the interferon-γ/STAT pathway. Nature 1999; 397(6721): 710-713
32. Border WA, Noble NA, Yamamoto T, Harper JR, Yamaguchi Y, Pierschbacher MD, et al. Natural inhibitor of transforming growth factor-beta protects against scarring in experimental kidney disease. Nature 1992, 360(6402): 361-364
33. Jiang Z, You DY, Chen XC, Wu J. Monitoring of serum markers for fibrosis during CCl4-induced liver damage. Effects of antifibrotic agents. J Hepatol 1992, 16(3):282-289
34. Fort J, Pilette C, Veal N, Oberti F, Gallois Y, Douay O, Rosenbaum J, Cales P. Effects of long-term administration of interferon in two models of liver fibrosis in rats. J Hepatol 1998, 29(2): 263-270
35. Bissell DM. Cell-matrix interaction and hepatic fibrosis. Prog Liver Dis 1990; 9:143-155
36. Friedman SL. Molecular regulation of hepatic fibrosis, an integrated cellular response to tissue injury. J Bio Chem 2000, 275(4): 2247-2250
37. Zhang LH, Liu CX, Yao HP, Chen H, Li MW. Intrahepatic expression of transforming growth factor and its receptor in rat hepatic fibrosis. J Zhejiang Univ (Medic Sci) 2000; 29(3):97-100

Received: June 20, 2009 / Accepted: November 25, 2009

Address for correspondence:
Prof. Lihuang Zhang, M.D.
Institute of Immunology
Zhejiang University School of Medicine
388 Yuhangtang Road
Hangzhou 310058
P.R. China
E-mail: zhanglihuang@zucc.edu.cn